

Influence of characteristics of the crystal structure of Nd_2CuO_4 on its magnetic properties

V. A. Blinkin, I. M. Vitebskii, O. D. Kolotii, N. M. Lavrinenko, V. P. Seminozhenko, and V. L. Sobolev

"Monokristallreaktiv" Scientific and Industrial Consortium
(Submitted 5 July 1990)

Zh. Eksp. Teor. Fiz. **98**, 2098–2109 (December 1990)

The increased interest in Nd_2CuO_4 arises primarily because this compound is the basis of a new class of high-temperature superconducting materials. Pure Nd_2CuO_4 exhibits a whole sequence of phase transitions, including a structural one and a number of magnetic transitions. A symmetry approach is used in the present study to investigate the relationships between characteristics of the crystal structure and the magnetic ordering of this compound. The normal modes of homogeneous oscillations of the spin system are determined. The symmetry of the spin-lattice coupling is analyzed. A linear magnetoelectric effect of exchange origin is predicted.

1. CRYSTAL SYMMETRY OF Nd_2CuO_4

Below room temperature the crystal structure of Nd_2CuO_4 can be described by the Fedorov group $I4/mmm$ and is presented in Fig. 1. The Cu^{2+} ions occupy a -type positions and form a body-centered tetragonal lattice. The Nd^{3+} ions occupy a pair of positions of the e type. According to Ref. 1, a continuous structural phase transition occurs at $T = T_c > 300$ K and its result is the displacement of the copper ions, as shown in Fig. 2.

Our standard group-theoretical analysis shows that structural distortions presented in Fig. 2 correspond to an active two-dimensional irreducible representation of the Fedorov group $I4/mmm$, which belongs to a two-ray $K13$ star (point X in the Brillouin zone). The disymmetric phase belongs to the Fedorov group $P4_2/mnm$ of the tetragonal system and has a primitive cell whose volume is four times as large as in the initial phase (Fig. 3). The main features of the group-theoretical analysis of the structural phase transition are given in the Appendix.

Magnetic ordering occurs in Nd_2CuO_4 in the disymmetric crystalline phase. In the sections below we analyze the very unusual magnetic properties of this compound. We concentrate our attention on the question of the extent to which any particular magnetic property is related to crystal structure distortions.

2. MAGNETIC ORDERING OF Nd_2CuO_4

Neutron diffraction investigations^{1,2} revealed three types of antiferromagnetic ordering of the magnetic moments of the copper ions in Nd_2CuO_4 , two of which are presented in Fig. 4 and the third in Fig. 5. The ranges of existence of these phases on the temperature scale are shown schematically in Fig. 6. All these magnetic configurations are realized in the disymmetric crystal phase (and they correspond to identical magnetic and crystallographic cells). The magnetic symmetry and the magnetic class of each of the three phases are

$$\text{AF-1: } P4_2/m'n'm', D_{4h}(D_4), \quad (1)$$

$$\text{AF-2: } P4_2'/m'nm', D_{4h}(D_{2d}), \quad (2)$$

$$\text{AF-3: } Pnnm', D_{2h}(C_{2v}). \quad (3)$$

The magnetic moments of the neodymium sublattices were detected only in the AF-3 phase for $T < 1.5$ K. Assuming that the magnetic "polarization" of the neodymium sublattices is not spontaneous, but due to the influence of the magnetically ordered copper subsystem [this is the assumption used in determination of the magnetic symmetry groups given by Eqs. (1)–(3)], we find that the symmetry considerations make it possible to determine how the magnetic moments of the neodymium ions are oriented. We can readily show that each of the three phases represents the x - y projections of the magnetic moments of the Nd ions located along one and the same c axis; these moments are ferromagnetically ordered and oriented in the same way as the spins of the copper ions on the same c axis (Fig. 1). The z projections of the magnetic moments of the Nd ions have opposite signs for

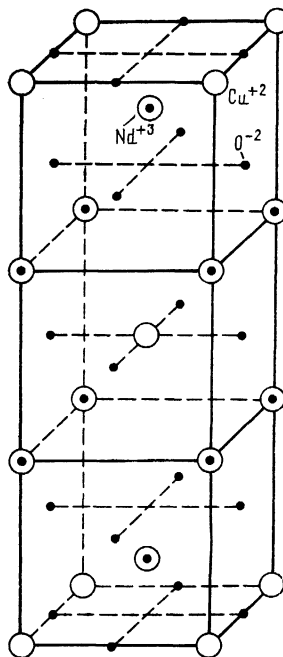


FIG. 1. Body-centered tetragonal cell of Nd_2CuO_4 in the high-symmetry phase.

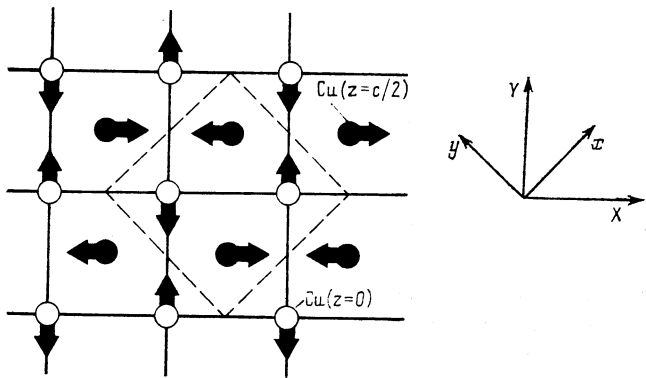


FIG. 2. Displacements of the copper ions as a result of a structural phase transition in Nd_2CuO_4 . The dashed square represents a primitive cell of the disymmetric phase. X , Y and x , y are, respectively, the old and new Cartesian axes.

the nearest neighbors along the c axis. The magnetic moments of the copper ions are all oriented entirely in the basal plane.

The role of the rare-earth subsystem in the formation of the magnetic properties of Nd_2CuO_4 can be identified only if we have information on the nature of the quantum states of the Nd^{3+} ions in the crystal field. Unfortunately, such information is not yet available. Naturally, an explicit allowance for the magnetic subsystem of neodymium has no effect on the results of the symmetry analysis. However, at sufficiently low temperatures there are additional branches in the spectrum of the spin excitations and these are associated with the rare-earth sublattices. We allow implicitly for the rare-earth magnetic subsystem via renormalization of the constants of the spin–spin and spin–lattice coupling of the copper ions.

3. SYMMETRY OF THE SPIN-SPIN INTERACTIONS IN Nd_2CuO_4

We are interested only in homogeneous states of the magnetic subsystem, i.e., states with $\mathbf{k} = 0$. The Hamiltonian of the spin–spin interactions can then be represented by a sum of the exchange and relativistic terms

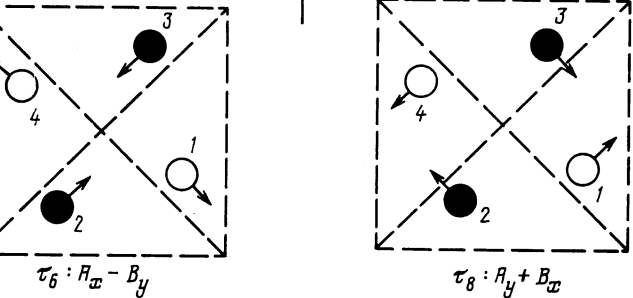


FIG. 4. Four types of planar exchange-noncollinear magnetic structures. According to Ref. 1, Nd_2CuO_4 exhibits the phases τ_2 (AF-1) and τ_8 (AF-2).

of the spin–spin interactions can then be represented by a sum of the exchange and relativistic terms

$$\mathcal{H}_s = \mathcal{H}_s^{(e)} + \mathcal{H}_s^{(a)}, \quad (4)$$

where the exchange contribution $\mathcal{H}_s^{(e)}$ to the energy of the spin–spin interactions is

$$\mathcal{H}_s^{(e)} = \sum_{\alpha, \alpha'} J_{\alpha\alpha'} \mathbf{S}_{\alpha} \mathbf{S}_{\alpha'} + \mathcal{H}_s^{(e)} (S^4). \quad (5)$$

The index α labels the magnetic sublattices of copper and, in accordance with Fig. 3, it has four values. The last term in Eq. (5) describes a biquadratic exchange, which is of fundamental importance for the compound under consideration.

In this and subsequent sections we investigate the ground states and homogeneous oscillations of the spin system. As a preliminary step, we represent the Hamiltonian of

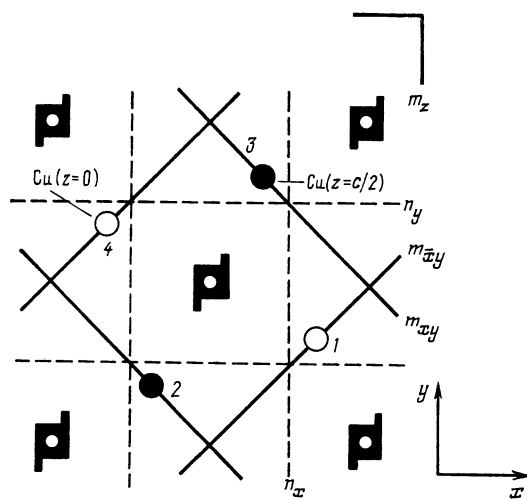


FIG. 3. Distribution of the symmetry elements of the space group $P4_2/mnm$. The positions of the copper ions in a primitive cell of the disymmetric phase are shown.

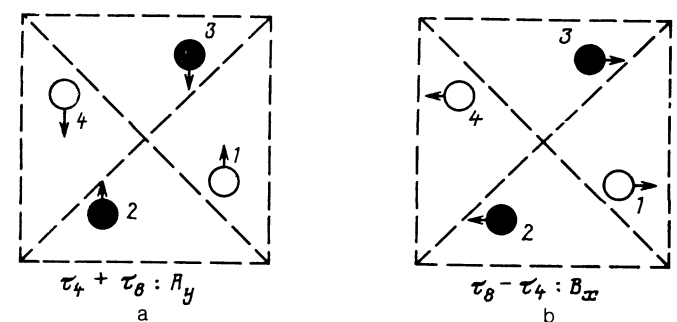


FIG. 5. Two equivalent collinear antiferromagnetic structures. According to Refs. 1 and 2, these phases occur at temperatures $T < 1.5$ K.

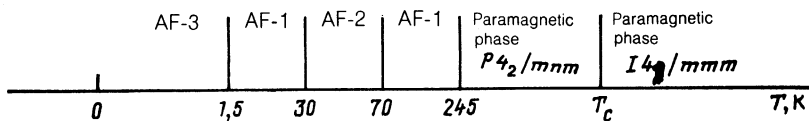


FIG. 6. Sequence of phases exhibited by Nd_2CuO_4 , shown on the increasing temperature scale.^{1,2}

Eq. (4) in a form which makes the symmetry of the system as clear as possible.

Following the standard procedure, we replace the spin moments of the individual sublattices S_x ($x = 1, 2, 3, 4$) with their linear combinations which realize irreducible representations of the group of transpositions of the atoms, i.e., we adopt the following ferromagnetic and antiferromagnetic vectors:

$$\begin{aligned} A &= S_1 + S_2 - S_3 - S_4, \quad C = S_1 - S_2 - S_3 + S_4, \\ B &= S_1 - S_2 + S_3 - S_4, \quad F = S_1 + S_2 + S_3 + S_4. \end{aligned} \quad (6)$$

The transformation properties of the vectors of Eq. (6) are given in Table I. This table gives the distribution, in terms of the irreducible representations of the group D_{4h}^{14} , of the quantities which are quadratic functions of the spins and also of the components of the strain tensor and of the electric polarization vector. All of them will be needed later.

In our calculations we employ the usual normalization (equal-magnitude) conditions:

$$S_1^2 = S_2^2 = S_3^2 = S_4^2 = S^2, \quad (7)$$

or in the equivalent form:

$$A^2 + B^2 + C^2 + F^2 = 16 S^2, \quad (8)$$

$$AB + FC = AC + BF = AF + BC = 0.$$

Using the data of Table I and the normalization conditions of Eq. (8), we obtain the following expression for the exchange part (5) of the Hamiltonian of Eq. (4):

$$\mathcal{H}_s^{(e)} = J_0(A^2 + B^2) + J_1 F^2 + D(A^2 - B^2)^2, \quad (9)$$

where J_0 and J_1 are the constants of the exchange interaction which is a quadratic function of the spins, whereas D is the biquadratic exchange constant. Equation (9) does not include the exchange invariant C^2 , because its inclusion in accordance with Eq. (8) simply renormalizes the constants J_0 and J_1 . Here and below we assume that the spin-spin interactions of different types are linked by the inequality

$$J \gg D \gg a, \quad (10)$$

where J , D , and a are, respectively, the quadratic exchange, biquadratic exchange, and anisotropy constants.

In the exchange approximation, when the conditions

$$J_0 < 0, \quad J_1, \quad D > 0 \quad (11)$$

are obeyed, the ground state of the spin system is characterized by a noncollinear (canted) but coplanar magnetic structure

$$AB = 0, \quad A^2 = B^2 = 8S^2, \quad (12)$$

whose orientation in the spin space is determined in turn by the anisotropic relativistic interactions $\mathcal{H}_s^{(a)}$. Using the data in Table I, as well as the conditions (8) and (10), we find that $\mathcal{H}_s^{(a)}$ is described by the following expression:

$$\mathcal{H}_s^{(a)} = a_2(A_x + B_y)^2 + a_4(A_y - B_x)^2 + a_6(A_x - B_y)^2 + a_8(A_y + B_x)^2. \quad (13)$$

Thus the orientation (in the spin space) of the exchange magnetic structure [Eq. (12)] is described by four independent parameters, which are second-order anisotropy constants. Note that inclusion of the contribution $A_z^2 + B_z^2$ to

TABLE I. Transformation properties of spin and macroscopic variables under transformations of the symmetry group $P4_2/mnm \rightarrow D_{4h}^{14}$ of the paramagnetic phase (\hat{u} is the strain tensor and \mathbf{p} is the electric polarization vector).

D_{4h}^{14}	S_x	$S_x S_{x'}$	$u_{\alpha\beta}$	\mathbf{p}
τ_1	—	$F^2, C^2, A^2 + B^2$	$u_{zz}, u_{xx} + u_{yy}$	—
τ_3	F_z	—	—	—
τ_5	C_z	$A^2 - B^2$	$u_{xx} - u_{yy}$	—
τ_7	—	FC, AB	u_{xy}	—
τ_9	$\begin{cases} F_x & C_y \\ F_y & C_x \end{cases}$	—	$\begin{cases} u_{yz} \\ -u_{xz} \end{cases}$	—
τ_2	$A_x + B_y$	—	—	—
τ_4	$A_y - B_x$	—	—	p_z
τ_6	$A_x - B_y$	—	—	—
τ_8	$A_y + B_x$	—	—	—
τ_{10}	$\begin{cases} B_z \\ -A_z \end{cases}$	$\begin{cases} FA \\ FB \end{cases} \begin{cases} CB \\ CA \end{cases}$	—	$\begin{cases} p_x \\ p_y \end{cases}$

$\mathcal{H}_s^{(a)}$ reduces to renormalization of the terms already written down, so that the corresponding term is omitted from Eq. (13).

If even one out of four constants a_n in Eq. (13) is negative, then in the ground state the magnetic moments of the copper sublattices are in the basal plane. Four inequivalent antiferromagnetic configurations are then possible (their stability ranges are indicated in parentheses):

$$\tau_2: A_x = B_y = \sqrt{8} S, P4_2/m'n'm' \quad (a_2 < 0, a_4, a_6, a_8), \quad (14)$$

$$\tau_4: A_y = -B_x = \sqrt{8} S, P4_2/m'n'm \quad (a_4 < 0, a_2, a_6, a_8), \quad (15)$$

$$\tau_6: A_x = -B_y = \sqrt{8} S, P4_2'/m'n'm \quad (a_6 < 0, a_2, a_4, a_8), \quad (16)$$

$$\tau_8: A_y = B_x = \sqrt{8} S, P4_2'/m'n'm' \quad (a_8 < 0, a_2, a_4, a_6). \quad (17)$$

They are shown in Fig. 4 as projections on the basal plane. However, if all these four constants are positive,

$$a_2, a_4, a_6, a_8 > 0, \quad (18)$$

the sublattice magnetizations of copper are tilted out of the basal plane and one of the mixed (irreducible) magnetic configurations is realized. According to the authors of Refs. 1 and 2, this situation does not occur in Nd_2CuO_4 .

Ordering of the magnetic moments of the copper ions lying in the same xy plane is governed by the antiferromagnetic exchange interaction between the nearest neighbors in this plane, i.e., by the exchange parameters $J_{14} = J_{23} < 0$ of Eq. (5). The simplest "chessboard" antiferromagnetic ordering is then established in the xy planes. The mutual orientation of the spins in the neighboring xy planes (i.e., in the planes separated from one another by $c/2$) is governed by the much weaker biquadratic exchange. This is because the interplanar exchange interaction, which is a quadratic function of the spins, is fully canceled when the ordering within the planes is of the chessboard type. In other words, the exchange parameters $J_{13} = J_{12} = J_{34} = J_{24}$ of Eq. (5), representing the interplanar exchange interaction, do not occur in the expression for the energy of the magnetic configurations characterized by $\mathbf{F} = \mathbf{C} = 0$. This reason alone allows us to represent the investigated magnetic structures as a superposition of two weakly coupled antiferromagnetic subsystems with the antiferromagnetic vectors

$$\mathbf{L}_1 = \mathbf{S}_1 - \mathbf{S}_4 = \frac{1}{2}(\mathbf{A} + \mathbf{B}), \quad \mathbf{L}_2 = \mathbf{S}_2 - \mathbf{S}_3 = \frac{1}{2}(\mathbf{A} - \mathbf{B}). \quad (19)$$

In the exchange approximation the mutual orientation of the vectors \mathbf{L}_1 and \mathbf{L}_2 is due to the biquadratic exchange interaction:

$$D(A^2 - B^2)^2 = 16D(\mathbf{L}_1 \cdot \mathbf{L}_2)^2. \quad (20)$$

In principle, we can assume that the anisotropic relativistic interactions of Eq. (13) could be comparable in magnitude with or even exceed the interplanar biquadratic exchange interaction of Eq. (20). In this case it is the relativistic interactions that determine the orientation of the vectors \mathbf{L}_1 and \mathbf{L}_2 .

We now return to the antiferromagnetic structures described by Eqs. (14)–(17) and shown in Fig. 4. First of all, we note that the geometry of these structures is described by Eqs. (14)–(17) exactly, irrespective of whether the inequalities of Eq. (10) are satisfied or whether the equal-magnitude conditions in Eq. (8) are obeyed. All four structures are characterized by the same exchange energies, because the

angles between the corresponding sublattice magnetizations are the same in all of them.

In principle, the magnetic structures of Eqs. (14)–(17) can exist also in the absence of the spontaneous distortions of the crystal structure which appear below T_c . However, we can easily show that in this case the magnetic configurations τ_2 and τ_6 are equivalent (are domains), and this is true of the magnetic configurations τ_4 and τ_8 . It follows that only two out of the four anisotropy constants in Eq. (13) are independent:

$$a_2 = a_6, \quad a_4 = a_8. \quad (21)$$

The equilibrium and hf magnetic properties of a system with this symmetry had already been investigated.^{3–5}

We now consider the collinear antiferromagnetic structure of Eq. (3) shown in Fig. 5a. A structure of the A_y type is equivalent to an antiferromagnetic structure of the B_x type shown in Fig. 5b (they are both domains). Moreover, these two structures are characterized by the same magnetic symmetry group $Pnnm'$, so that neither of them can be realized in its pure form: they should always accompany one another. The latter follows also from the invariance of the bilinear form $A_x B_y$. Nevertheless, the low-temperature phase AF-3 can be nearly collinear. In fact, if we use the hierarchy of Eq. (10) for the spin–spin interactions, we find that the magnetic structures shown in Fig. 5 are realized

$$D < 0, \quad a_4 + a_8 < 0, \quad a_2 + a_6. \quad (22)$$

In the exchange approximation they are exactly collinear, but if we allow for the relativistic interactions we find, in accordance with Eqs. (13) and (20), that there are two equivalent solutions for the ground state:

$$1) \quad A_y \approx 4S, \quad B_x \approx \frac{a_8 - a_4}{8|D|S}, \quad 2) \quad B_x \approx 4S, \quad A_y \approx \frac{a_8 - a_4}{8|D|S}. \quad (23)$$

The proximity of these magnetic structures to collinearity may be due to two independent factors. First, it may be due to predominance of the biquadratic exchange interaction over the relativistic contributions. Second, according to Eq. (21), the difference $a_8 - a_4$ in Eq. (23) is due to spontaneous distortions of the crystal structure. If the role of these distortions is slight, we may indeed find that

$$|a_8 - a_4| \ll |a_8|, |a_4|, \quad |a_2 - a_6| \ll |a_2|, |a_6|. \quad (24)$$

We conclude this section by noting that an explicit allowance for the rare-earth subsystem is needed to go beyond the framework of the pure symmetry approach in an analysis of the magnetic properties of the low-temperature phase. Because of the absence of reliable experimental data this is not yet possible. Therefore, in the next section dealing with the spin dynamics we consider only the phases AF-1 and AF-2.

4. HOMOGENEOUS OSCILLATIONS OF THE SPIN SYSTEM

We begin with the assumption that at moderately low temperatures the role of the rare-earth magnetic subsystem reduces to renormalization of the parameters of the spin Hamiltonian of the copper magnetic subsystem. In this case the exchange-noncollinear (anted) phases of Eqs. (14)–(17) are each characterized by four antiferromagnetic reso-

TABLE II. Classification of homogeneous oscillations of the spin system and of components of the strain tensor \hat{u} and of the electric polarization vector \mathbf{p} under irreducible representations of the unitary subgroup D_4 of the point group of the magnetic symmetry of the τ_2 (AF-1) phase.

D_4	$S_{\mathbf{x}}$	\hat{u}	\mathbf{p}	Normal modes
A_1	$A_x + B_y$	$u_{zz}, u_{xx} + u_{yy}$	—	—
A_2	$A_y - B_x, F_z$	—	p_z	a_1
B_1	$A_x - B_y, C_z$	$u_{xx} - u_{yy}$	—	e
B_2	$A_y + B_x$	u_{xy}	—	—
E	$\begin{cases} F_x \\ F_y \end{cases}, \begin{cases} C_y \\ C_x \end{cases}, \begin{cases} B_z \\ -A_z \end{cases}$	$\begin{cases} u_{yz} \\ -u_{xz} \end{cases}$	$\begin{cases} p_x \\ p_y \end{cases}$	$a2$ $a3$

nance modes of which one is an exchange mode and the other three are acoustic. The structure and the symmetry of all the normal modes of homogeneous oscillations of the spin system are described in Tables II-V. The frequencies of these modes are given by the following expressions.

The exchange mode (in all the phases $\tau_2 - \tau_8$) has the frequency

$$\omega_e = (8S)^2 (-J_0 D)^{1/2}. \quad (25)$$

The acoustic mode frequencies are as follows:

$$\text{phase } \tau_2: \quad \begin{cases} \omega_{a1} = 8S[2(a_2 - a_4)(J_0 - J_1)]^{1/2}, \\ \omega_{a2} = \omega_{a3} = 8S[a_2(2J_0 - J_1)]^{1/2}, \end{cases} \quad (26)$$

$$\text{phase } \tau_4: \quad \begin{cases} \omega_{a1} = 8S[2(a_4 - a_2)(J_0 - J_1)]^{1/2}, \\ \omega_{a2} = \omega_{a3} = 8S[a_4(2J_0 - J_1)]^{1/2}, \end{cases} \quad (28)$$

$$\text{phase } \tau_6: \quad \begin{cases} \omega_{a1} = 8S[2(a_6 - a_8)(J_0 - J_1)]^{1/2}, \\ \omega_{a2} = \omega_{a3} = 8S[a_6(2J_0 - J_1)]^{1/2}, \end{cases} \quad (30)$$

$$\text{phase } \tau_8: \quad \begin{cases} \omega_{a1} = 8S[2(a_8 - a_6)(J_0 - J_1)]^{1/2}, \\ \omega_{a2} = \omega_{a3} = 8S[a_8(2J_0 - J_1)]^{1/2}. \end{cases} \quad (32)$$

The above expressions for the frequencies are derived using the inequalities of Eq. (10). The degeneracy of the acoustic modes $a2$ and $a3$ is exact in all the phases. The unusually low frequency ω_e of the exchange mode, which is related to the role of the biquadratic exchange interaction in the formation of magnetic structures, is also noteworthy. An analogous situation occurs also in UO_2 (Ref. 6).

The last column in Tables II-V gives the classification of the homogeneous oscillations of the spin system in accordance with irreducible representations of the unitary subgroup of the magnetic symmetry group of each of the phases $\tau_2 - \tau_8$. The rest of the notation in Tables II-V is identical with the notation used in Table I. The first column in these tables gives the symbol of the irreducible representation. The second column lists the irreducible combination of the sublattice magnetizations. The third and fourth columns of Tables II-V give the transformation properties of the components of the strain tensor \hat{u} and of the electric polarization vector \mathbf{p} , relative to the transformations from the unitary subgroups applicable for magnetic configurations. These tables describe the structure of all the antiferromagnetic resonance modes and allow for the method of excitation of each of the modes.

We now give a specific example. It follows from Table II that an acoustic magnon $a1$ in the $\tau_2(\text{AF-1})$ phase is asso-

TABLE III. Same as Table II, but for the τ_4 phase.

C_{4v}	$S_{\mathbf{x}}$	\hat{u}	\mathbf{p}	Normal modes
A_1	$A_y - B_x$	$u_{zz}, u_{xx} + u_{yy}$	p_z	—
A_2	$A_x + B_y, F_z$	—	—	a_1
B_1	$A_y + B_x, C_z$	$u_{xx} - u_{yy}$	—	e
B_2	$A_x - B_y$	u_{xy}	—	—
E	$\begin{cases} F_x \\ F_y \end{cases}, \begin{cases} C_y \\ C_x \end{cases}, \begin{cases} B_z \\ -A_z \end{cases}$	$\begin{cases} u_{yz} \\ -u_{xz} \end{cases}$	$\begin{cases} p_x \\ p_y \end{cases}$	$a2$ $a3$

TABLE IV. Same as Table II, but for the τ_6 phase.

D_{2d}	s_x	\dot{u}	p	Normal modes
A_1	$A_x - B_y$	$u_{zz}, u_{xx} + u_{yy}$	—	—
A_2	$A_y + B_x, F_z$	—	—	$a1$
B_1	$A_x + B_y, C_z$	$u_{xx} - u_{yy}$	—	e
B_2	$A_y - B_x$	u_{xy}	p_z	—
E	$\begin{cases} F_x \\ -F_y \end{cases}, \begin{cases} C_y \\ -C_x \end{cases}, \begin{cases} B_z \\ -A_z \end{cases}$	$\begin{cases} u_{yz} \\ u_{xz} \end{cases}$	$\begin{cases} p_x \\ p_y \end{cases}$	$a2$ $a3$

ciated with oscillations of the spin variables $A_y - B_x$ and F_z . This magnon can be excited by an oscillating magnetic field H_z or by an oscillating electric field E_z . Degenerate acoustic magnons $a2$ and $a3$ are excited in the same phase by a magnetic field $H \perp z$, by an electric field $E \perp z$, and by transverse sound accompanied by the strains u_{xz} or u_{yz} . Finally, an exchange magnon e can be excited only by transverse sound, accompanied by the strains $u_{xx} - u_{yy}$. Similar information on the phases τ_4 , τ_6 , and τ_8 can be found in Tables III–V.

5. SPIN-LATTICE INTERACTION AND TENSOR PROPERTIES OF MAGNETICALLY ORDERED PHASES

It is well known that the presence of a magnetic order can alter qualitatively the macroscopic (tensor) properties of a crystal. In particular, the spin-lattice coupling may give rise to such phenomena specific to magnetically ordered crystals as the linear piezomagnetic or magnetoelectric effects, etc. The symmetry of the tensor properties is determined uniquely by the magnetic class. In particular, the magnetic symmetry groups of all the antiferromagnetic structures listed in Figs. 4 and 5 admit the existence of the linear magnetoelectric effect. The exchange noncollinear structures of Eqs. (14)–(17) are of particular interest from this point of view. In such cases the linear magnetoelectric effect is of exchange origin and, consequently, can be particularly large. According to Table I, the following invariant is responsible for the exchange magnetoelectric effect:

$$p_x \mathbf{FA} + p_y \mathbf{FB}. \quad (34)$$

Linerization of the spin part of Eq. (34) with respect to small deviations from the ground state gives the following expressions for the phases $\tau_2 - \tau_8$:

$$\text{phase } \tau_2: \sqrt{8} S(p_x F_z + p_y F_y), \quad (35)$$

$$\text{phase } \tau_4: \sqrt{8} S(p_x F_y - p_y F_x), \quad (36)$$

$$\text{phase } \tau_6: \sqrt{8} S(p_x F_z - p_y F_y), \quad (37)$$

$$\text{phase } \tau_8: \sqrt{8} S(p_x F_y + p_y F_z). \quad (38)$$

We must stress once again that the magnetoelectric effect occurring in these phases is determined by the strongest exchange part of the spin-lattice coupling.

In the collinear phase (Fig. 5) the interaction of Eq. (34) also induces the linear magnetoelectric effect, which is of exchange origin. However, in this case the exchange effect is due to breakdown of the equal-magnitude condition of Eq. (8). At low temperatures equal-magnitude condition of the rare-earth magnetic subsystem should be disobeyed, so that the influence of the rare earth is in this case dominant.

It is important to stress that the magnetoelectric effect in all the magnetic structures mentioned above is also due to the existence of spontaneous distortions of the crystal structure that appear below T_c . In fact, in the absence of such distortions, we would expect antitranslations in the antiferromagnetic structures shown in Figs. 4 and 5. We recall that

TABLE V. Same as Table II, but for the τ_8 (AF-2) phase.

D'_{2d}	s_x	\dot{u}	p	Normal modes
A_1	$A_y + B_x$	$u_{zz}, u_{xx} + u_{yy}$	—	—
A_2	$A_x - B_y, F_z$	—	—	$a1$
B_1	$A_x + B_y$	u_{xy}	—	—
B_2	$A_y - B_x, C_z$	$u_{xx} - u_{yy}$	p_z	e
E	$\begin{cases} F_y \\ -F_x \end{cases}, \begin{cases} C_x \\ C_y \end{cases}, \begin{cases} B_z \\ -A_z \end{cases}$	$\begin{cases} u_{xz} \\ +u_{yz} \end{cases}$	$\begin{cases} p_x \\ p_y \end{cases}$	$a2$ $a3$

TABLE VI. Matrices of the irreducible representation responsible for the structural phase transition at $T = T_c$.

\hat{g}	$1, m_z$	$\bar{1}, 2_z$	$4_z, \bar{4}_z^3$	$4_z^*, \bar{4}_z$	$2_X, m_Y$	$2_Y, m_X$	$2_{XY}, m_{\bar{X}Y}$	$2_{\bar{X}Y}, m_{XY}$
$D(g)$	$(1 \ 0)$	$(-1 \ 0)$	$(0 \ 1)$	$(1 \ -1)$	$(0 \ 1)$	$(-1 \ 0)$	$(-1 \ 0)$	$(1 \ -1)$

the occurrence of antitranslations in the magnetic symmetry group is incompatible with the linear magnetoelectric and piezomagnetic effects.⁷

The authors are grateful to A. S. Borovik-Romanov, V. V. Eremenko, V. I. Ozhogin, and L. A. Prozorova for valuable discussions and encouragement.

APPENDIX. GROUP-THEORETICAL ANALYSIS OF A STRUCTURAL PHASE TRANSITION IN Nd_2CuO_4

The structural phase transition which occurs in this compound below T_c is characterized by a two-dimensional irreducible representation of the Fedorov group $I4/mmm$, which belongs to a two-ray star $K13$ with the following rays:

$$\mathbf{k} = \frac{\mathbf{b}_3}{2} = \frac{\pi}{a}(\mathbf{e}_x + \mathbf{e}_y); \quad \mathbf{k} = \frac{\mathbf{b}_1 - \mathbf{b}_2}{2} = \frac{\pi}{a}(\mathbf{e}_y - \mathbf{e}_x) = \hat{4}_z \mathbf{k}_1. \quad (\text{A1})$$

Here, \mathbf{e}_α are the Cartesian unit vectors; $\hat{4}_z$ is the operation of rotation by an angle $\pi/2$ about the z axis; \mathbf{b}_i are the reciprocal lattice vectors (the notation adopted here is basically the same as that used in the handbook of Kovalev⁸). The same irreducible star is responsible for the structural phase transition reported for La_2CuO_4 in Ref. 9, but in contrast to La_2CuO_4 , a two-ray transition channel applies in the case of Nd_2CuO_4 . Consequently, the translation symmetry of the disymmetric phase Nd_2CuO_4 is governed by the following triplet of the primitive translations that form the simple tetragonal lattice:

$$\begin{aligned} \mathbf{a}_1' &= a(\mathbf{e}_x + \mathbf{e}_y) = \mathbf{a}_1 + \mathbf{a}_2 + 2\mathbf{a}_3, \\ \mathbf{a}_2' &= a(\mathbf{e}_y - \mathbf{e}_x) = \mathbf{a}_1 - \mathbf{a}_2 = \hat{4}_z \mathbf{a}_1', \\ \mathbf{a}_3' &= c\mathbf{e}_z = \mathbf{a}_1 + \mathbf{a}_2, \end{aligned} \quad (\text{A2})$$

where \mathbf{a}_i' are the primitive translations of the initial base-centered tetragonal lattice.

It should be noted that in the case of the phase transition characterized by the two-beam channel of the star $K13$ the disymmetric phase unavoidably suffers also from distortions corresponding to a one-ray star $K15$ with a single ray

$$\mathbf{k} = \mathbf{k}_1 + \mathbf{k}_2 = 2 \frac{\pi}{a} \mathbf{e}_y = 2 \frac{\pi}{a} \mathbf{e}_x = \frac{\mathbf{b}_1 - \mathbf{b}_2 + \mathbf{b}_3}{2}, \quad (\text{A3})$$

where as usual the symbol $\ll \equiv \gg$ means equality of the wave vectors (apart from the reciprocal lattice vector). However, in the case of the phase transition in Nd_2CuO_4 it is found that the distortions corresponding to the star $K15$ do not occur in the mechanical representation of the crystal, i.e., they do not result in displacements of the ions.

Table VI lists the matrices of the irreducible representation responsible for the structural phase transition at T_c . The operations \hat{g} of the Fedorov group $I4/mmm$ correspond to elements of the zeroth block. The basis functions ψ_1 and ψ_2 , transforming in accordance with the first and second rows of the matrix $D(g)$, correspond to the wave vectors \mathbf{k}_1 and \mathbf{k}_2 from Eq. (A1). The copper ion displacements shown in Fig. 2 correspond to the solution

$$\psi = \eta_1 \psi_1 + \eta_2 \psi_2, \quad \eta_1 = \eta_2. \quad (\text{A4})$$

The corresponding Fedorov group of the disymmetric phase is $P4_2/mnm$, described in Fig. 3. Throughout this paper, with the exception of Eqs. (A1)–(A3) and Table VI, the Cartesian coordinate axes x and y are parallel to the primitive translations \mathbf{a}_1' and \mathbf{a}_2' of the disymmetric phase.

¹ S. Skanthakumar, H. Zhang, T. W. Clinton *et al.*, Physica C (Utrecht) **160**, 124 (1989).

² M. J. Rosseinsky and K. Prassides, Physica C (Utrecht) **162–164**, 522 (1989).

³ I. M. Vitebskii and N. M. Lavrinenco, Fiz. Tekh. Vys. Davlenii No. 24, 3 (1987).

⁴ V. G. Bar'yakhtar, I. M. Vitebskii, Yu. G. Pashkevich *et al.*, Zh. Eksp. Teor. Fiz. **87**, 1028 (1984) [Sov. Phys. JETP **60**, 587 (1984)].

⁵ N. M. Lavrinenco, *Author's Abstract of Doctoral Thesis* [in Russian], Kharkov (1990).

⁶ I. E. Dzyaloshinskii and B. G. Kukhareno, Zh. Eksp. Teor. Fiz. **75**, 2290 (1978) [Sov. Phys. JETP **48**, 1155 (1978)].

⁷ L. D. Landau, E. M. Lifshitz, and L. P. Pitaevskii, *Electrodynamics of Continuous Media*, 2nd ed., Pergamon Press, Oxford (1984).

⁸ O. V. Kovalev, *Irreducible and Induced Representations and Corepresentations of the Fedorov Groups* [in Russian], Nauka, Moscow (1986), p. 141.

⁹ N. M. Plakida and V. S. Shakhmatov, Physica C (Utrecht) **153–155**, 233 (1988).

Translated by A. Tybulewicz